J-3-3

Extended Abstracts of the 2011 International Conference on Solid State Devices and Materials, Nagoya, 2011, pp1195-1196

Device Performance of Graphene Nanoribbon MOSFET and Tunneling FET with Phonon Scattering: A Computation Study

Kai-Tak Lam[1*], Sai-Kong Chin[2], and Gengchiau Liang[1,2†]

[1]Dept. of Electrical and Computer Engineering, National University of Singapore, 4 Engineering Drive 3, Singapore 117576
[2]Institute of High Performance Computing, Fusionopolis, 1 Fusionopolis Way, #16-16 Connexis, Singapore 138632
Phone: +65-6516 2898 E-mail: *lamkt@nus.edu.sg, †elelg@nus.edu.sg

1. Introduction

Research in carbon electronics has been intensified since 2004 and in particular the use of graphene nanoribbon (GNR) in digital devices has been widely explored. While many studies of the GNR metal-oxide-semiconductor field-effect transistors (MOSFET) [1]-[3] and tunneling FET (TFET) [4], [5] has discuss their device performance in the ballistic limits individually, few studies have compared their characteristics with the consideration of phonon scattering [6], [7]. In this study, we present our investigation of the device performance of GNR MOSFET and TFET using a non-equilibrium Green's function (NEGF) quantum simulator with a mode-space Dirac equation model. We observed that in the presence of phonon scattering, both the OFF-state and ON-state currents (I_{OFF} and I_{ON}) of MOSFET are degraded, and the I_{ON} of TFET was enhanced. We also examined the effect of channel length (L_C) on the device performances in the presence of phonon scattering and we observed that the I_{ON} of MOSFET is more degraded by increasing L_C than that of TFET.

2. Methodology

A schematic of the device simulated in this study is shown in Fig. 1(a). A GNR of width 1.0 nm is chosen, with an energy bandgap of 0.87 eV. The source is n-type doped for MOSFET and p-type doped for TFET and the drain is n-type doped for both devices. The doping concentration is 4.47×10^{13} cm^{-2} for both n- and p-type doping. The device has a double metal gate structure with silicon dioxide as the insulating material. The retarded Green's function G^r in the NEGF formulism is obtained from [8]

$$G^r = \left[EI + i\eta - H_0 - U - \Sigma_S - \Sigma_D - \Sigma_{ph}\right]^{-1}. \qquad (1)$$

The device Hamiltonian H_0 is described with the mode-space Dirac equation [4] and the Σ_S and Σ_D are the self-energies of the source and drain. The phonon scattering is incorporated in the simulator via Σ_{ph} which is obtained by the sum of in- and out-scattering self-energies calculated based on the self-consistent Born approximation [8], [9]

$$\Sigma_{ph}^{in/out}(E) = \int \Big\{ D^{ab}(\hbar\omega)\left[N(\hbar\omega)+1\right] G^{n/p}(E \pm \hbar\omega) + D^{em}(\hbar\omega) N(\hbar\omega) G^{n/p}(E \mp \hbar\omega) \Big\} d\omega. \qquad (2)$$

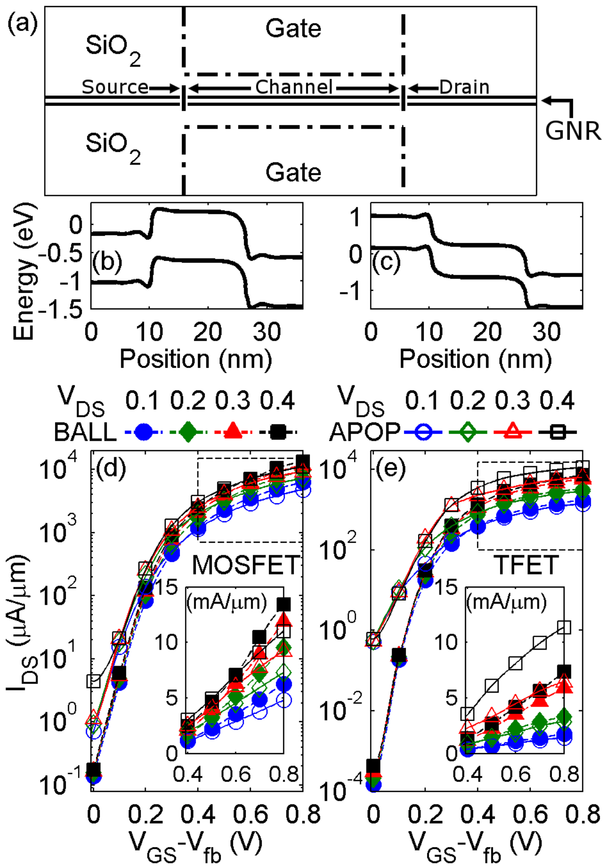

Fig. 1 (a) Schematic of the device simulated. The oxide thickness (t_{ox}) is 1 nm and the gate thickness (t_{gate}) is 3 nm. The band diagram along the device transport direction at V_{DS} = 0.4 V and V_{GS}-V_{fb} = 0 V are shown in (b) and (c) for GNR MOSFET and TFET, respectively. The V_{fb} is the flat band potential due to the metal gate work function and is set to be 0.2 V here. The transfer characteristics of GNR MOSFETS and TFET for ballistic (BALL) and phonon scattering (APOP) regimes are shown in (d) and (e), respectively. Insets show the linear plots at high gate biases.

The electron-phonon coupling constants $D^{ab} = D^{em} = D$ is obtained following Ref. 6 and for acoustic phonon (AP), $D_{AP} = 3.1\times10^{-3}$ eV^2 and for optical phonon (OP), assuming only phonon energy $\hbar\omega$ = 0.19 eV is significant, D_{OP} = 1.30×10^{-2} eV^2. N is the phonon occupation number from the Bose-Einstein distribution at room temperature and $G^{n/p}$ is the electron/hole correlation function [8]. The potential U is calculated self-consistently by a 2D Poisson solver [5].

3. Results and discussion

The transfer characteristics of the GNR MOSFET and TFET are shown in Fig. 1(a) and 1(b) respectively with different V_{DS}, with L_C = 16 nm. For MOSFET, the phonon scattering increased the I_{OFF} and decreased the I_{ON}, with 76%-82% ballisticity. However, the I_{OFF} of TFET was increased by 4 orders while the I_{ON} for V_{DS} = 0.4 V was nearly doubled. In order to understand the different effect of phonon scattering on the devices, the IV and the current flux plots of the devices under V_{DS} = 0.4 V are plotted in Fig. 2 and 3 for GNR MOSFET and TFET, respectively.

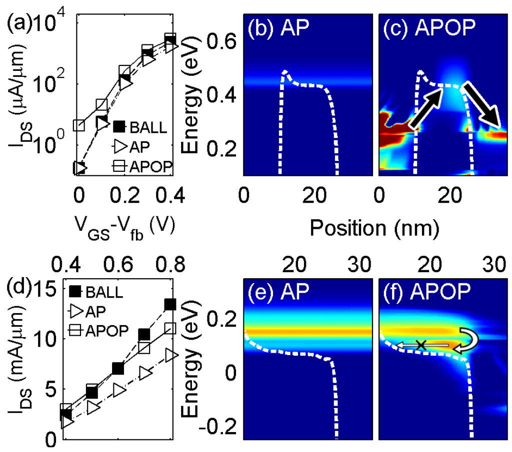

Fig. 2 (a) The IV of MOSFET at V_{DS} = 0.4 V at low gate biases. (b) and (c) show the current flux plots at V_{GS}-V_{fb} = 0 V. (d) The IV of MOSFET at high gate biases and (e) and (f) show the current flux plots at V_{GS}-V_{fb} = 0.8 V. The arrows show phonon emission (downwards) and absorption (upwards).

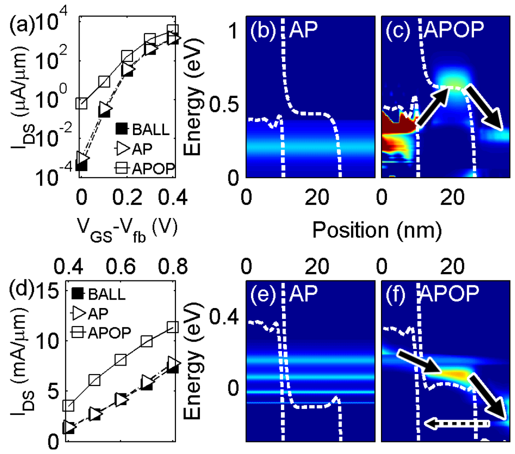

Fig. 3 (a) The IV of TFET at V_{DS} = 0.4 V at low gate biases. (b) and (c) show the current flux plots at V_{GS}-V_{fb} = 0 V. (d) The IV of TFET at high gate biases and (e) and (f) show the current flux plots at V_{GS}-V_{fb} = 0.8 V. In (f), the dash arrow indicates a small current flowing from drain to source due to the huge accumulation of charges, reducing the total current. This 'back tunneling' current is reduced for larger channel length.

For GNR MOSFET, AP scattering did not affect the currents at low gate biases [Fig. 2(a)] due to the high barrier where only a very small current was present, and hence back scattering was not apparent. However, OP scattering increased the amount of carrier at the source by phonon absorption and a larger I_{OFF} was observed [Fig. 2(c)]. At higher gate biases, the back scattering reduced the current significantly [Fig. 2(d)]. Conversely, OP scattering reduced the back scattering by bringing down the carriers' energy via phonon emission in the channel [Fig. 2(f)] and the current was restored. However, the I_{ON} was still lower than the ballistic values due to a finite amount of back scattering.

For GNR TFET, AP scattering did not affect the current at all gate biases [Fig. 3(a) & 3(d)] due to the higher carrier concentration at the source than the channel, which prohibited back scattering. On the other hand, OP scattering enhanced band-to-band tunneling (BTBT) [Fig. 3(c) & 3(f)] which increased the current significantly. In the presence of OP scattering, BTBT between source and channel became the dominant mechanism even for I_{OFF} [Fig. 3(c)].

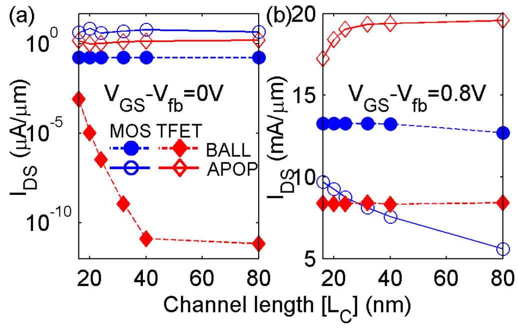

Fig. 4 The channel length dependence of (a) I_{OFF} and (b) I_{ON}.

Lastly, the effect of L_C for GNR MOSFET and TFET was investigated and the I_{OFF} (V_{GS}-V_{fb} = 0 V) and I_{ON} (V_{GS}-V_{fb} = 0.8 V) as a function of LC is plotted in Fig. 4. While the I_{OFF} of both devices increased with phonon scattering, the I_{OFF} of TFET was still lower than MOSFET. It was noted that the ballistic I_{OFF} for TFET was decreasing with increasing L_C, as the dominant mechanism was BTBT between source and drain. With phonon scattering, BTBT occurs between the source and channel and hence I_{OFF} remained invariant. The I_{ON} of GNR MOSFET decreased with increasing L_C due to the increased back scattering and since AP scattering had minimal effect on GNR TFET, the I_{ON} was in general not affected by L_C. However, due to the accumulation of charges at the drain, a minute amount of carrier tunneling from the drain to the source occurs [Fig. 3(f)]. As L_C increased, this 'back tunneling' was reduced and hence the I_{ON} increased initially.

References

[1] G. Liang, *et al.*, IEEE Trans. Elec. Dev. 54, 677 (2007).
[2] G. Fiori, *et al.*, IEEE Elec. Dev. Lett. 28, 760 (2007).
[3] Y. Yoon, *et al.*, Appl. Phys. Lett. 98, 203503 (2011).
[4] S.-K. Chin, *et al.*, IEEE Trans. Elec. Dev. 57, 3144 (2010).
[5] K.-T. Lam, *et al.*, IEEE Elec. Dev. Lett. 32, 431 (2011).
[6] Y. Ouyang, *et al.*, Appl. Phys. Lett. 92, 243124 (2008).
[7] S. O. Koswatta, *et al.*, IEEE Trans. Elec. Dev. 56, 456 (2009)
[8] S. Datta, *Quantum Transport* (2005) Chapter 10
[9] D. Nikonov, *et al.*, (2009) http://nanohub.org/resources/7772.